Available online at www.sciencedirect.com
ScienceDirect
Trans. Nonferrous Met. Soc. China 32(2022) 1061−1069
Transactions of Nonferrous Metals Society of China
www.tnmsc.cn

Effect of trace boron on grain refinement of commercially pure aluminum by Al−5Ti−1B

Fei XIAO[1], Ming-xu WU[1], Yi-xiao WANG[2], Wen-zhe ZHOU[1], Shu-bin WANG[1], Dong-hong WANG[1], Guo-liang ZHU[1], Michael JIANG[3], Da SHU[1], Jia-wei MI[4], Bao-de SUN[1]

1. Shanghai Key Lab of Advanced High-temperature Materials and Precision Forming and State Key Laboratory of Metal Matrix Composites, School of Materials Science and Engineering, Shanghai Jiao Tong University, Shanghai 200240, China;
2. National Engineering Research Center of Light Alloy Net Forming, School of Materials Science and Engineering, Shanghai Jiao Tong University, Shanghai 200240, China;
3. Shenzhen Almate Inc., Shenzhen 518102, China;
4. School of Engineering and Computer Science, University of Hull, Hull, HU6 7RX, UK

Received 27 April 2021; accepted 26 September 2021

Abstract: The effect of boron content on grain refinement of commercially pure aluminum by Al−5Ti−1B was quantitatively assessed. When the boron content is less than 0.03 wt.%, the refining performance of Al−5Ti−1B gradually is weakened as the boron content increases, which is attributed to the reaction of boron with the Al_3Ti interlayer on TiB_2 and the consumption of solute Ti. On the contrary, when the boron content exceeds 0.03 wt.%, the refining performance of Al−5Ti−1B gradually recovers with increasing boron content, which is related to the formation of primary AlB_2 particles that provide additional nucleant substrates.
Key words: aluminum alloy casting; Al−5Ti−1B; grain refinement; boron treatment; nucleation

1 Introduction

Owing to the low density, excellent electrical conductivity and good formability, aluminum alloys have been widely used to produce electric wires and cables [1−3]. Unfortunately, the transition metal (TM) elements such as V, Ti, Cr, and Zr usually serve as impurities in commercially pure aluminum, causing severe lattice distortion of Al metal matrix, which increases electron scattering and damages electrical conductivity [4,5]. As an economical and time-saving way, boron treatment is widely used to improve the conductivity by converting these impurities into non-metal borides [6].

Alloy strength, which can be improved by refining grains according to the Hall−Petch relationship [7,8], should also be considered for the application of aluminum alloy wires. It has been reported that the combination of grain refinement and boron treatment can improve the mechanical properties and electrical conductivity of Al alloys simultaneously [9,10].

The addition of Al−5Ti−1B grain refiner, containing TiB_2 particles and solute Ti, has been commonly used to obtain a fine grain size in aluminum industry for decades [11−13]. Normally, the grain size of commercial aluminum can be reduced from millimeter scale to ~200 μm with only 0.1 wt.% Al−5Ti−1B addition [14]. It is well accepted that TiB_2 is a potent nucleant particle to promote heterogeneous nucleation, which is

Corresponding author: Da SHU, Tel: +86-21-54742683, E-mail: dshu@sjtu.edu.cn
DOI: 10.1016/S1003-6326(22)65855-2

considered to be the main reason of the refinement [15−18]. Moreover, excessive Ti is also essential for grain refinement due to its strong segregation ability [17], which provides constitutional supercooling and restrains grain growth [19]. As reported by FAN et al [12] and LI et al [20], the enriched layer of Ti atoms was observed and Al_3Ti two-dimensional compound (2DC) was formed on the surface of TiB_2 particles during nucleation. According to the Bramfitt's equation [21], the lattice mismatch degree between Al_3Ti and α(Al) is only 0.9%, which is far less than that between TiB_2 and α(Al) (5.9%). As suggested by HIRATA and HIRANO [22], nucleation can be easier because of the lower interfacial energy caused by the lower lattice mismatch. Evidenced by other studies, Al−Ti−B grain refiners can hardly refine the grains of pure aluminum without excessive solute Ti [13], which further explains the important role of solute Ti during refinement. However, boron treatment may reduce solute Ti in melt and impair the grain refining effect significantly, which occurs frequently in industry practice but has not been given sufficient attention. In this study, quantitative assessment of B content on the performance of Al−5Ti−1B grain refiner was conducted and its underlying mechanism was discussed. This work contributes to understanding the grain refinement mechanism of Al−5Ti−1B refiner for Al alloys containing trace boron.

2 Experimental

2.1 Casting

Seven aluminum alloy ingots containing different B contents (1#: 0B, 2#: 0.005 B, 3#: 0.01 B, 4#: 0.02 B, 5#: 0.03 B, 6#: 0.05 B and 7#: 0.1 B, in wt.%, if not stated otherwise) were prepared using commercially pure aluminum (CP-Al, 99.7% purity) and Al−3B master alloy in a resistance furnace. The CP-Al and the Al−3B master alloy were melted at 730 °C and held for 1 h firstly, then 0.2% commercial Al−5Ti−1B rods (9.5 mm in diameter, provided by Aleastur Company in Spain) enveloped within an aluminum-foil was added to the melt at 730 °C and held for 10 min. Subsequently, the melt was stirred with a graphite rod for 30 s, poured into a Reynolds standard golf tee mold (Fig. 1) preheated at 200 °C and cooled in the air. In this work, excessing Ti and B in the melt were provided by Al−5Ti−1B and Al−3B master alloys, respectively. Inductively coupled plasma (ICP) was used to determine the actual chemical compositions of the ingots, and the results are shown in Table 1.

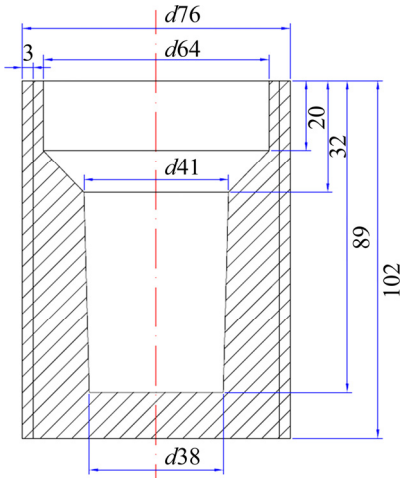

Fig. 1 Sketch of Reynolds standard golf tee mold (unit: mm)

Table 1 Actual chemical compositions of ingots (wt.%)

Sample	Ti	B	Al
1#	0.0089	0	Bal.
2#	0.0096	0.0053	Bal.
3#	0.0112	0.0108	Bal.
4#	0.0108	0.0225	Bal.
5#	0.0093	0.0316	Bal.
6#	0.0096	0.0524	Bal.
7#	0.0099	0.1035	Bal.

2.2 Metallography

The section at a distance of 51 mm from the bottom of the ingot was polished and etched with Keller reagent (5 mL HF + 20 mL HCl + 20 mL HNO_3 + 20 mL H_2O) to observe the macrographs. The pixel analysis method in Photoshop software was used to measure the proportion of the equiaxed crystal region in the macrographs. And the specimens for microstructure analysis were obtained by anodic oxidation in 2.5 vol.% HBF_4 solution and observed with an OLYMPUS polarizing microscope. In order to ensure the accuracy, 10 areas were randomly selected from the micrographs to measure the average grain size of equiaxed regions.

2.3 Thermodynamic calculation

In order to determine the existing forms of Al,

Ti and B in the melt, the calculation of Al−Ti−B ternary equilibrium phase diagram was performed using the Pandat software.

2.4 Characterization

To determine the binding state among elements in CP-Al ingots containing 0.02% B and 0.03% B, X-ray photoelectron spectroscopy (XPS) analysis was conducted. In order to extract particles in the ingots for XPS analysis, 100 g samples with different B contents were immersed in 20 vol.% HCl solution for 50 h to ensure the dissolution of Al. A scanning electron microscope (SEM, Quanta−200) equipped with an energy dispersive X-ray spectroscope (EDS) was used to identify the composition of particles in ingots.

3 Results and discussion

3.1 Metallographic observation

Figure 2 clearly presents the macrographs of aluminum ingots containing different B contents inoculated with 0.2% Al−5Ti−1B and corresponding optical micrographs of the central region. The measured proportions of the equiaxed grain area to the total area, and average equiaxed grain sizes of the aluminum ingots with different B contents are shown in Fig. 3. In all cases, an inner equiaxed grain region is surrounded by an outer columnar grain region, but different contents of B element change the relative area percentages of the equiaxed grain regions dramatically. With the increase of B content (up to 0.02%), the area proportion of equiaxed crystal decreases remarkably, while the average equiaxed grain size increases significantly, as shown in Figs. 2(a−d) and Fig. 3. In the case of 0.02% B, it exhibits a nearly complete columnar macrostructure as shown in Fig. 2(d), indicating that the columnar to equiaxed transition (CET) was inhibited by B addition. However, with further increase of B content to 0.1%, the equiaxed grain zone is enlarged while the average equiaxed grain size decreases gradually, as shown in Figs. 2(e−g) and Fig. 3, showing that the CET tends to be easier when the B content increases above 0.03%.

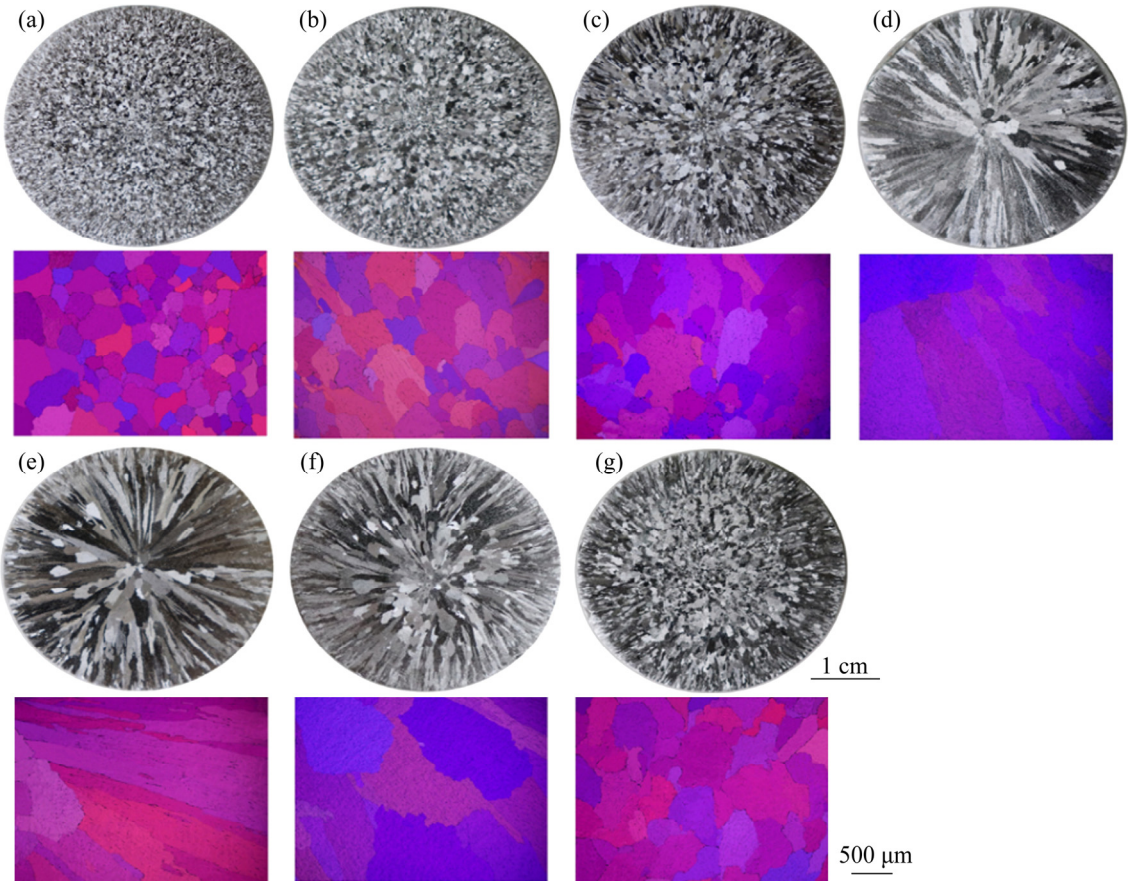

Fig. 2 Macrographs and micrographs of CP-Al ingots showing effect of B content on grain refining efficiency of Al−5Ti−1B: (a) 0% B; (b) 0.005% B; (c) 0.01% B; (d) 0.02% B; (e) 0.03% B; (f) 0.05% B; (g) 0.1% B

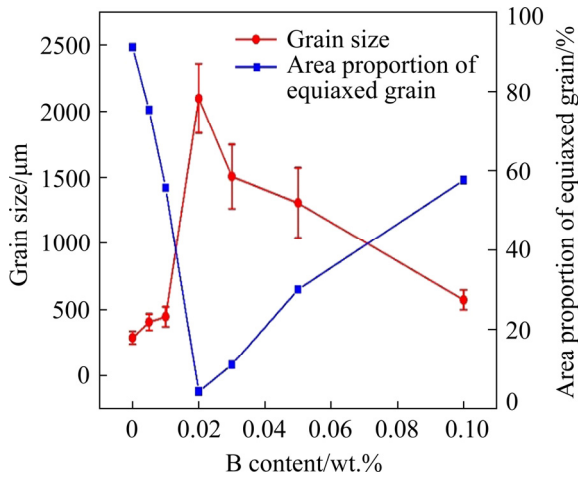

Fig. 3 Evolution of proportion of equiaxed grain area to total area, and average equiaxed grain size with different B contents

3.2 Thermodynamic calculation

In order to determine the binding state among Al, Ti and B at 720 °C, the standard Gibbs free energies of formation (ΔG) for the compounds (TiB_2, AlB_2 and Al_3Ti) were obtained from the previous report (Table 2) [23]. It can be seen that the order of ΔG is $TiB_2 < AlB_2 < Al_3Ti < 0$, indicating that Ti and B are much easier to form stable boride TiB_2 in the Al−Ti−B ternary system. The excessive B in the melt comes from the Al−3B master alloy. After the Al−5Ti−1B refiner is added to the melt, Al_3Ti is dissolved and excessive Ti is released into the melt [23]. Since the Gibbs free energy of TiB_2 is more negative than that of AlB_2 and Al_3Ti, Ti in the melt tends to combine with B to form TiB_2.

Table 2 Comparison of Gibbs free energies of formation (ΔG) for TiB_2, AlB_2 and Al_3Ti at 720 °C [23]

Compound	Al_3Ti	AlB_2	TiB_2
ΔG/(kJ·mol^{-1})	−128	−155	−342

In order to further determine the existing forms of Al, Ti and B in the ternary system at 720 °C, phase diagram calculation was performed. In our experiments, the only source of Ti in aluminum is the Al−5Ti−1B refiner, and the final Ti content is ~0.01%. It can be seen from Fig. 4 that TiB_2 is stable in the melt. When the B content reaches ~0.03%, AlB_2 is formed as the primary phase in the melt.

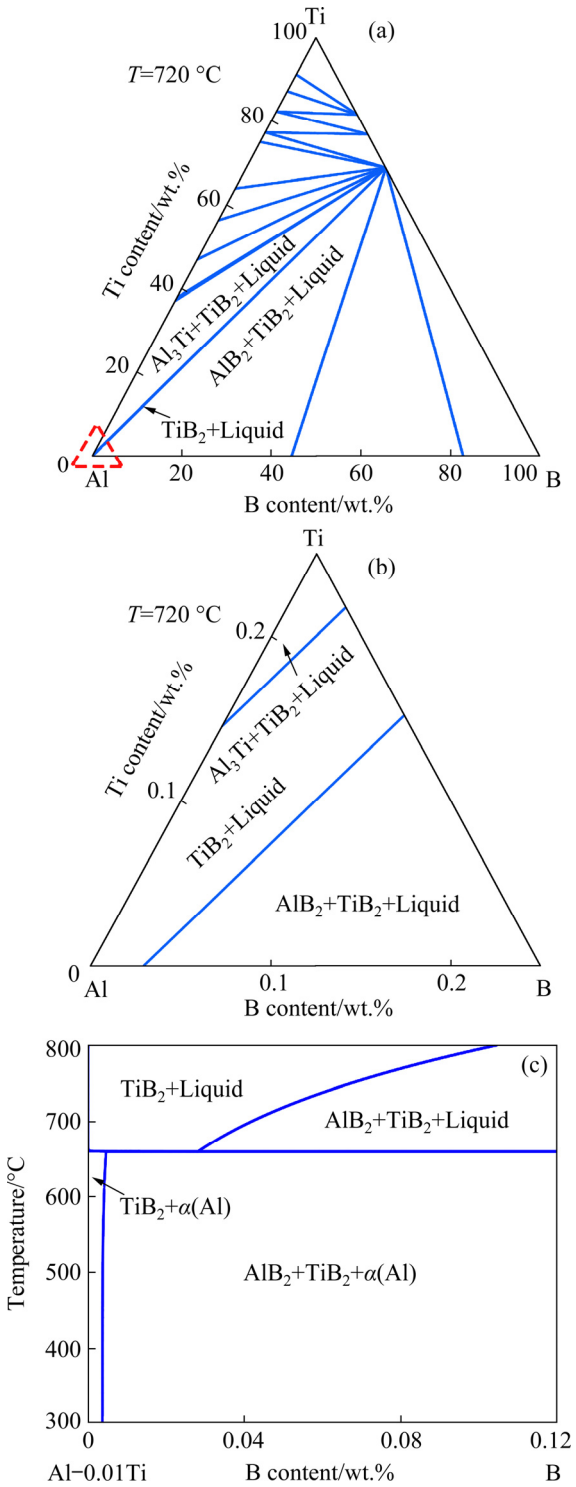

Fig. 4 Thermodynamic calculation results of Al−Ti−B system: (a) Ternary phase diagram of Al−Ti−B; (b) Enlarged diagram of Al-richened corner in (a); (c) Vertical section at 0.01% Ti

3.3 Effects of boron on grain refinement

3.3.1 Boron content lower than 0.03%

As reported by FAN et al [12] and LI et al [20], the enriched layer of Ti atoms was

observed and Al_3Ti (2DC) was formed on the surface of TiB_2 particles during nucleation. According to the Bramfitt's equation [21], the lattice mismatch degree between Al_3Ti and α(Al) is only 0.9%, which is far less than that between TiB_2 and α(Al) (5.9%). As proposed by TURNBULL and VONNEGUT [24], the nucleation undercooling ΔT_n is related to the lattice mismatch δ, expressed by the following equation:

$$\Delta T_n = \frac{C_E}{\Delta S_V}\delta^2 \quad (1)$$

where C_E is the coefficients of elasticity, and ΔS_V is the entropy of phase transition per volume. It can be inferred that the enrichment of Ti at the interface between TiB_2 and Al promotes the nucleation. When the B content is less than 0.03%, excessive B exists in the melt in the form of B atoms. The reaction between B and Ti atoms may destroy the enriched layer of Ti atoms and inhibit the formation of Al_3Ti (2DC) on the surface of TiB_2 particles, resulting in the deterioration of nucleation ability of TiB_2.

On the other hand, the growth restriction effect of Ti element is also one of the factors affecting the refining effect of the Al−5Ti−1B master alloy. The effect of solute elements on grain growth can be quantitatively expressed by the growth restriction factor Q [17,18,25,26]. The value of Q is related to the liquidus slope m_l and the equilibrium partition coefficient k [19,25,27]:

$$Q=m_lC_0(k-1) \quad (2)$$

where C_0 is the element composition in wt.%.

Table 3 [19,28] gives the relative Q values of Ti and B elements at the same C_0. The Q value of element Ti is two orders of magnitude higher than that of element B under the same solute concentration. When the Al−5Ti−1B refiner was added to the melt containing boron, due to the stability of TiB_2, a part of B atoms reacted with the excessive Ti solute to form TiB_2 and thus the total value of Q was reduced. Therefore, as the B content increased up to 0.02%, the decrease in both the nucleation ability of TiB_2 particles and the growth restriction effect of solute led to the reduction of equiaxed crystal area, as shown in Figs. 2(a−d).

3.3.2 Boron content higher than 0.03%

It is worth noting that the refining performance of Al−5Ti−1B gradually recovers when the B content is higher than 0.03% (Fig. 2). Based on the phase diagrams in Fig. 4, AlB_2 appears as the primary phase crystallized from the melt when the B content is higher than 0.03%. As shown in Fig. 5, the XPS results show that only Ti—B peak [29] and O—B peak [30] exist in the sample with 0.02% B, while Al—B peak [30] appears in the sample containing 0.03% B, indicating the presence of AlB_2 when the content of B exceeds 0.02%. The O—B peak may be caused by incomplete cleaning during extraction.

Table 3 Comparison of relative values of Q for Ti and B elements at the same C_0

Element	Liquidus slope, m_l	Equilibrium distribution coefficient, k	$m_l(k-1)$
Ti [19]	33.3	7.67	222.1
B [28]	−34.2	0.45	18.8

Since TiB_2 is more stable than AlB_2 in the Al−Ti−B ternary system, when Al−5Ti−1B is added into Al−B melt (B content >0.03%), excessive Ti in Al−5Ti−1B may react with AlB_2 in the following order:

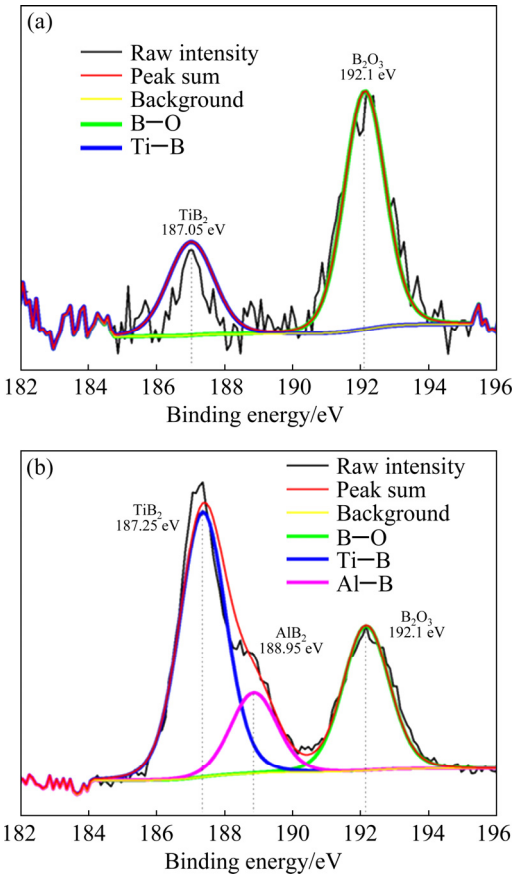

Fig. 5 XPS binding energy spectra for extracted particles from 0.02% B (a) and 0.03% B (b) samples

$$AlB_2+Ti\rightarrow(Al,Ti)B_2 \quad (3)$$

$$(Al,Ti)B_2+Ti\rightarrow TiB_2+Al \quad (4)$$

where $(Al,Ti)B_2$ exists in the melt as the intermediate product of $AlB_2 \rightarrow TiB_2$ reaction.

Figure 6 shows that the particles aggregate at the bottom of the 0.1% B sample, in which Ti signals were detected with EDS. The particle size in Fig. 6 is 20−30 μm, which is obviously larger than the size of TiB_2 particles in the Al−5Ti−1B refiner, indicating that those coarse particles are not TiB_2. Based on the above analysis, we deduce that the particles in Fig. 6 are AlB_2 and the intermediate phase $(Al,Ti)B_2$. Different from the direct reaction of solute Ti with B in the case of B content lower than 0.03%, Reactions (3) and (4) are very slow kinetically. Therefore, the consumption of Ti solute and the reaction between the Al_3Ti intermediate layer and B at nucleation interface may be weakened, which is helpful for the recovery of refinement effect.

Previous studies [31−33] have reported that AlB_2 can refine aluminum alloys when the B content increases above 0.022%. As shown in Fig. 7(a), the Al−3B master alloy contains AlB_2 compound. In order to study the refinement effect of AlB_2 on CP-Al, the macrostructure of CP-Al refined by the Al−3B master alloy containing AlB_2 particles was observed. Figure 7(b) shows that the Al−3B significantly reduces the grain size of CP-Al. According to the Bramfitt's equation [21], the lattice mismatch degree between AlB_2 and α(Al) is ~5.24%, close to that between TiB_2 and α(Al), which indicates that AlB_2 is also a potent nucleation site for α(Al).

In the current work, the size of AlB_2 or the intermediate $(Al,Ti)B_2$ is 2−30 μm (Fig. 6), which is much larger than TiB_2 in the Al−5Ti−1B (Fig. 8). GREER et al [11] proposed the following free growth model:

$$\Delta T_{c,n}=4\sigma_{SL}/(\Delta S_V d_p) \quad (5)$$

where $\Delta T_{c,n}$ represents the critical nucleation undercooling, σ_{SL} is the solid−liquid interface energy, and d_p is the particle diameter. Assuming the nucleation undercooling for AlB_2 or $(Al,Ti)B_2$ is close to that for TiB_2, the α(Al) crystals will preferentially nucleate on larger particles, so AlB_2 or $(Al,Ti)B_2$ acts as the nucleation substrate first. Therefore, the existence of AlB_2 or $(Al,Ti)B_2$ particles causes the recovery of refining effect when the B content is higher than 0.03%.

Based on the above analysis, the underlying mechanism of boron on the grain refinement of aluminum by Al−5Ti−1B can be demonstrated in Fig. 9. Normally, as shown in Fig. 9(a), TiB_2 particles with Al_3Ti interlayer act as potent nucleant substrates, and excessive Ti inhibits grain growth, which contributes to excellent grain refinement of CP-Al without B. When the B content is lower than 0.03%, the increase of B content weakens the refining effect of Al−5Ti−1B on CP-Al, because the doping of B on the Al_3Ti interlayer leads to the increase of lattice mismatch between Al_3Ti and α(Al) and impairs the nucleation ability of TiB_2 particles. In addition, a part of B reacts with excessive Ti solute in the melt and weakens the grain growth restriction effect of Ti, as shown in Fig. 9(b). However, with further increase of B content larger than 0.03%, the occurrence of AlB_2

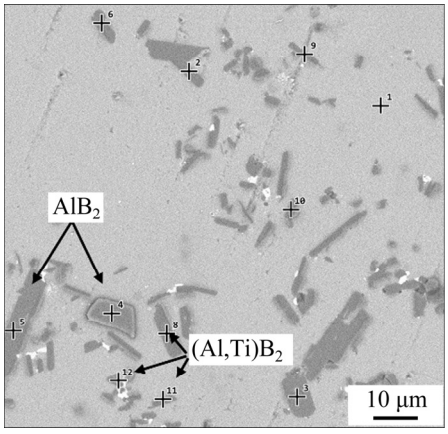

Element at Point 1	wt.%	Element at Point 3	wt.%	Element at Point 4	wt.%
Al	99.33	Al	91.51	Al	97.27
Ti	0.26	Ti	0.71	Ti	–
B	0.41	B	7.78	B	2.73

Element at Point 5	wt.%	Element at Point 8	wt.%	Element at Point 11	wt.%
Al	97.80	Al	91.89	Al	99.24
Ti	–	Ti	0.41	Ti	0.18
B	2.20	B	7.70	B	0.58

Fig. 6 Morphology and point energy spectrum results of particles at bottom of 0.1% B sample cooled in furnace

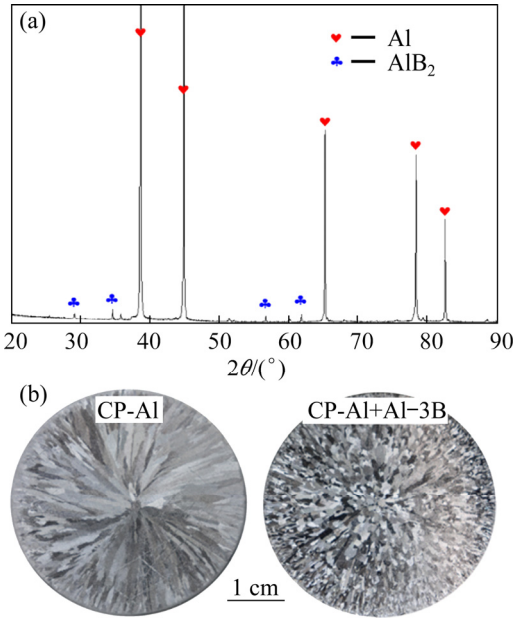

Fig. 7 XRD results of Al−3B master alloy (a) and macrostructures of CP-Al ingot without B and with 0.1% B (via addition of Al−3B master alloy) (b)

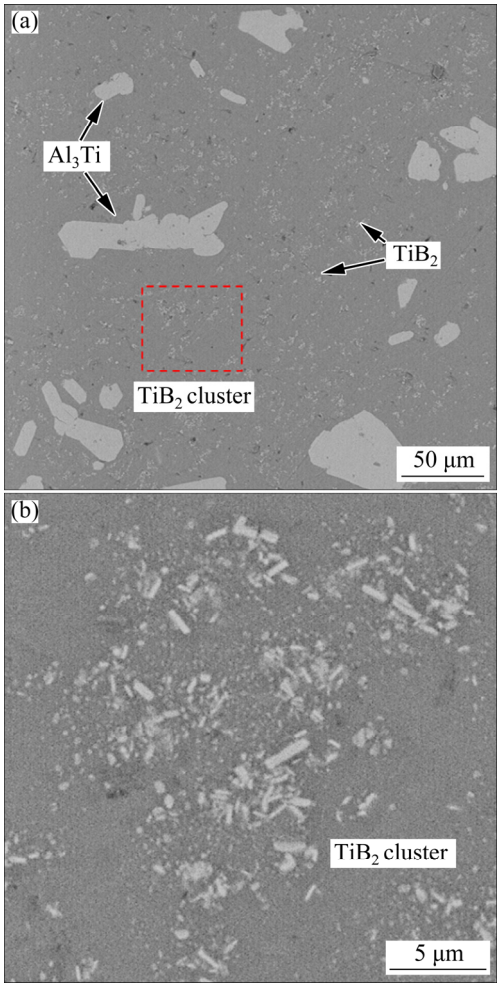

Fig. 8 Morphologies of Al−5Ti−1B refiner including Al_3Ti and TiB_2 (a), and enlarged TiB_2 cluster (b) in (a)

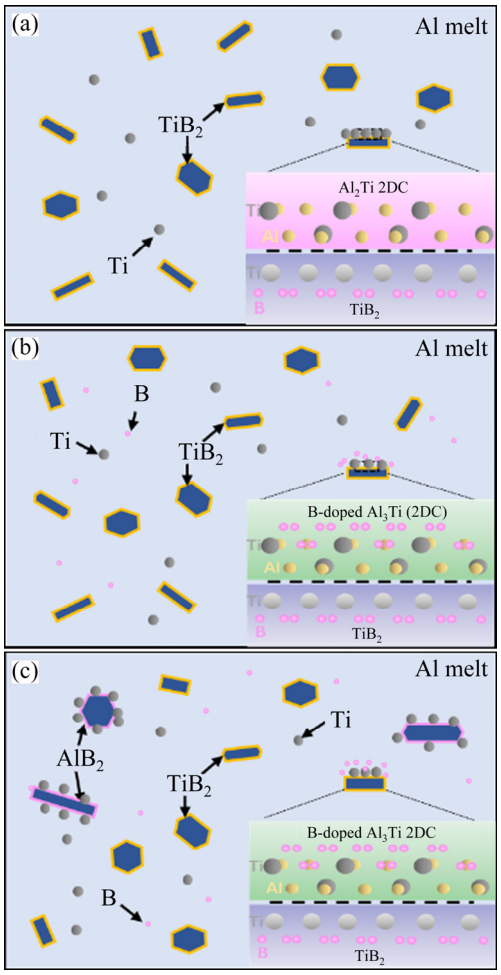

Fig. 9 Schematic diagrams showing mechanism of boron on nucleation of α(Al) in Al melt containing 0.2% Al−5Ti−1B refiner: (a) Without B; (b) B content lower than 0.03%; (c) B content higher than 0.03%

or the intermediate $(Al,Ti)B_2$ particles provide new substrates for the nucleation of aluminum, as shown in Fig. 9(c), resulting in the recovery of grain refinement of CP-Al.

4 Conclusions

(1) When the B content is less than 0.03%, with the increase of B content, the area proportion of equiaxed grain decreases while the average equiaxed-grain size increases. On the contrary, when the B content exceeds 0.03%, the grain refining effect of Al−5Ti−1B gradually recovers with further increase of B content.

(2) The main reason for the deleterious effect on grain refinement in the case of boron content lower than 0.03% is that the nucleation ability of TiB_2 particles is deteriorated due to the reaction

between B and Al_3Ti interlayer on TiB_2 particles and the growth restriction effect is weakened due to the consumption of solute Ti by B.

(3) The recovery of grain refining performance of Al−5Ti−1B in the case of boron content higher than 0.03% is mainly attributed to the formation of AlB_2 or intermediate phase $(Al,Ti)B_2$ acting as nucleant substrates.

Acknowledgments

The authors express their gratitude for the financial supports from the National Natural Science Foundation of China (Nos. U1832183, 52090042, 51821001).

References

[1] RODRIGUES A V, LIMA T S, VIDA T A, BRITO C, GARCIA A, CHEUNG N. Microstructure features and mechanical/electrochemical behavior of directionally solidified Al−6wt.%Cu−5wt.%Ni alloy [J]. Transactions of Nonferrous Metals Society of China, 2021, 31: 1529−1549.

[2] ZHAO Qing-ru, CUI Xiao-li, ZHAO Qian, LIU Xiang-fa. The synergistic effect of Al−B−C master alloy to improve conductivity and strength of 1070 alloy [J]. Journal of Alloys and Compounds, 2015, 639: 478−482.

[3] LIU C H, CHEN J, LAI Y X, ZHU D H, GU Y, CHEN J H. Enhancing electrical conductivity and strength in Al alloys by modification of conventional thermo-mechanical process [J]. Materials & Design, 2015, 87: 1−5.

[4] KARABAY S, UZMAN I. Inoculation of transition elements by addition of AlB_2 and AlB_{12} to decrease detrimental effect on the conductivity of 99.6% aluminium in CCL for manufacturing of conductor [J]. Journal of Materials Processing Technology, 2005, 160: 174−182.

[5] KHALIQ A, RHAMDHANI M A, BROOKS G A, GRANDFIELD J F. Removal of vanadium from molten aluminum — Part I. Analysis of VB_2 formation [J]. Metallurgical and Materials Transactions B: Process Metallurgy and Materials Processing Science, 2014, 45: 752−768.

[6] CUI Xiao-li, WU Yu-ying, CUI Hong-wei, ZHANG Guo-jun, ZHOU Bo, LIU Xiang-fa. The improvement of boron treatment efficiency and electrical conductivity of AA1070Al achieved by trace Ti assistant [J]. Journal of Alloys and Compounds, 2018, 735: 62−67.

[7] ASHTIANI H R R, SHAYANPOOR A A. New constitutive equation utilizing grain size for modeling of hot deformation behavior of AA1070 aluminum [J]. Transactions of Nonferrous Metals Society of China, 2021, 31: 345−357.

[8] DAHLE A K, ARNBERG L. Development of strength in solidifying aluminium alloys [J]. Acta Materialia, 1997, 45: 547−559.

[9] CUI Xiao-li, WU Yu-ying, ZHANG Guo-jun, LIU Yi-bo, LIU Xiang-fa. Study on the improvement of electrical conductivity and mechanical properties of low alloying electrical aluminum alloys [J]. Composites (Part B): Engineering, 2017, 110: 381−387.

[10] CUI Xiao-li, WU Yu-ying, LIU Xiang-fa, ZHAO Qing-ru, ZHANG Guo-jun. Effects of grain refinement and boron treatment on electrical conductivity and mechanical properties of AA1070 aluminum [J]. Materials & Design, 2015, 86: 397−403.

[11] GREER A L, BUNN A M, TRONCHE A, EVANS P V, BRISTOW D J. Modelling of inoculation of metallic melts: Application to grain refinement of aluminium by Al−Ti−B [J]. Acta Materialia, 2000, 48: 2823−2835.

[12] FAN Z, WANG Y, ZHANG Y, QIN T, ZHOU X R, THOMPSON G E, PENNYCOOK T, HASHIMOTO T. Grain refining mechanism in the Al/Al−Ti−B system [J]. Acta Materialia, 2015, 84: 292−304.

[13] XU Xue-xia, FENG Yan-ting, FAN Hui, WANG Qing, DONG Guo-zhen, LI Guo-wei, ZHANG Zi-han, LIU Qing, FAN Xiao-liang, DING Hai-min. The grain refinement of 1070 alloy by different Al−Ti−B mater alloys and its influence on the electrical conductivity [J]. Results in Physics, 2019, 14: 102482.

[14] ALAMDARI H D, DUBÉ D, TESSIER P. Behavior of boron in molten aluminum and its grain refinement mechanism [J]. Metallurgical and Materials Transactions A: Physical Metallurgy and Materials Science, 2013, 44: 388−394.

[15] ZHANG Li-li, JIANG Hong-xiang, HE Jie, ZHAO Jiu-zhou. Kinetic behaviour of TiB_2 particles in Al melt and their effect on grain refinement of aluminium alloys [J]. Transactions of Nonferrous Metals Society of China, 2020, 30: 2035−2044.

[16] HAN Yan-feng, DAI Yong-bing, SHU Da, WANG Jun, SUN Bao-de. Electronic and bonding properties of TiB_2 [J]. Journal of Alloys and Compounds, 2007, 438: 327−331.

[17] XU Y, CASARI D, DU Q, MATHIESEN R H, ARNBERG L, LI Y. Heterogeneous nucleation and grain growth of inoculated aluminium alloys: An integrated study by in situ X-radiography and numerical modelling [J]. Acta Materialia, 2017, 140: 224−239.

[18] EASTON M, STJOHN D. Grain refinement of aluminum alloys: Part I. The nucleant and solute paradigms—A review of the literature [J]. Metallurgical and Materials Transactions A: Physical Metallurgy and Materials Science, 1999, 30: 1613−1623.

[19] QUESTED T E, DINSDALE A T, GREER A L. Thermodynamic modelling of growth-restriction effects in aluminium alloys [J]. Acta Materialia, 2005, 53: 1323−1334.

[20] LI Yang, HU Bin, LIU Bin, NIE An-min, GU Qin-fen, WANG Jian-feng, LI Qian. Insight into Si poisoning on grain refinement of Al−Si/Al−5Ti−B system [J]. Acta Materialia, 2020, 187: 51−65.

[21] BRAMFITT B L. The effect of carbide and nitride additions on the heterogeneous nucleation behavior of liquid iron [J]. Metallurgical Transactions, 1970, 1: 1987−1995.

[22] HIRATA V M L, HIRANO K. Ostwald ripening of γ-Fe precipitates in a Cu−1.5at.%Fe alloy [J]. Scripta Metallurgica et Materialia, 1994, 31: 117−120.

[23] YUE N L, LU L, LAI M O. Application of thermodynamic calculation in the in-situ process of Al/TiB_2 [J]. Composite Structures, 1999, 47: 691−694.

[24] TURNBULL D, VONNEGUT B. Nucleation catalysis [J]. Industrial & Engineering Chemistry, 1952, 44: 1292−1298.
[25] MEN H, FAN Z. Effects of solute content on grain refinement in an isothermal melt [J]. Acta Materialia, 2011, 59: 2704−2712.
[26] FAN Z, GAO F, ZHOU L, LU S Z. A new concept for growth restriction during solidification [J]. Acta Materialia, 2018, 152: 248−257.
[27] XU H, XU L D, ZHANG S J, HAN Q. Effect of the alloy composition on the grain refinement of aluminum alloys [J]. Scripta Materialia, 2006, 54: 2191−2196.
[28] ZHANG Xiao-bo, ZHU Peng, ZENG Long, FENG Bai-gang, WAN Xiong-bin, REN Jun-qiang. Effect of adding Ce on the hot-tearing susceptibility of the $5TiB_2$/Al−5Cu composite [J]. Materials Characterization, 2020, 168: 110552.
[29] YANG Hua-bing, ZHAO Qian, ZHANG Guo-jun, NIE Jin-feng, LIU Xiang-fa. The grain refinement performance of B-doped TiC on Zr-containing Al alloys [J]. Journal of Alloys and Compounds, 2018, 731: 774−783.
[30] LU Xin-hong, LIU Wei, OUYANG Jun, TIAN Yun. Distinct surface hydration behaviors of boron-rich boride thin film coatings [J]. Applied Surface Science, 2014, 311: 749−752.
[31] VINOD KUMAR G S V, MURTY B S, CHAKRABORTY M. Settling behaviour of $TiAl_3$, TiB_2, TiC and AlB_2 particles in liquid Al during grain refinement [J]. International Journal of Cast Metals Research, 2010, 23: 193−204.
[32] ANTONIO J A M, LFO L F M. Grain refinement in aluminum alloyed with titanium and boron [J]. Metallurgical Transactions, 1971, 2: 465−471.
[33] WANG Tong-min, CHEN Zong-ning, FU Hong-wang, XU Jun, FU Ying, LI Ting-ju. Grain refining potency of Al−B master alloy on pure aluminum [J]. Scripta Materialia, 2011, 64: 1121−1124.

微量硼添加对 Al−5Ti−1B 细化工业纯铝的影响

肖 飞[1]，吴明旭[1]，王一笑[2]，周文哲[1]，王舒滨[1]，汪东红[1]，
祝国梁[1]，Michael JIANG[3]，疏 达[1]，米家伟[4]，孙宝德[1]

1. 上海交通大学 材料科学与工程学院 先进高温材料与精密成形上海市重点实验室和金属基复合材料国家重点实验室，上海 200240；
2. 上海交通大学 材料科学与工程学院 轻合金精密成型国家工程研究中心，上海 200240；
3. 深圳 Almate 有限公司，深圳 518102；
4. School of Engineering and Computer Science, University of Hull, Hull, HU6 7RX, UK

摘 要：定量研究硼含量对 Al−5Ti−1B 细化工业纯铝的影响。研究发现，当 B 含量低于 0.03% (质量分数)时，Al−5Ti−1B 的细化性能随 B 含量的增加而逐渐减弱，这是由于 B 与 TiB_2 上的 Al_3Ti 中间层发生反应以及熔体中溶质 Ti 的消耗。相反，当 B 含量超过 0.03% (质量分数)时，Al−5Ti−1B 的细化性能随着 B 含量的增加而逐渐恢复，这与熔体中 AlB_2 颗粒的形成有关，AlB_2 颗粒为 α(Al)的形核提供额外的形核核心。

关键词：铝合金铸造；Al−5Ti−1B；晶粒细化；硼化处理；形核

(Edited by Wei-ping CHEN)